J Solid State Electrochem (2004) 8: 655–660
DOI 10.1007/s10008-003-0490-9

ORIGINAL PAPER

E. D. Politova · S. Yu. Stefanovich · A. K. Avetisov
V. V. Aleksandrovskii · T. Yu. Glavatskih
N. V. Golubko · G. M. Kaleva · A. S. Mosunov
N. U. Venskovskii

Processing, structure, microstructure, and transport properties of the oxygen-conducting ceramics (La,Sr)(Ga,M)O_y (M=Mg, Fe, Ni)

Received: 11 April 2003 / Accepted: 29 September 2003 / Published online: 12 February 2004

Abstract The structure, microstructure, and dielectric and transport properties of (La,Sr)(Ga,M)O_y (M = Mg, Fe, and Ni) ceramic solid solutions have been studied by X-ray diffraction, thermogravimetry, and dilatometry in various gas atmospheres. Enhancement of conductivity and an increase of the thermal expansion coefficient have been confirmed to correlate with an increasing concentration of oxygen vacancies at high temperatures in the samples studied. Transformation from pure ionic to mixed conductivity has been revealed in the samples with increasing iron or nickel content.

Keywords Perovskite structure · Fe- and Ni-substituted lanthanum gallate · Thermal expansion · Mass loss · Dc and ac conductivity

Introduction

Investigations of ionic and mixed conducting oxides attract much attention due to the prospects of their applications as catalysts, sensors, solid electrolytes, materials, etc. [1, 2, 3, 4]. Moreover, mixed conducting membranes are also known to be key elements of the new technologies of natural and off-gas conversion [5]. During recent years, intensive efforts have been devoted to the search for mixed conducting multicomponent oxides that meet the demands for membranes exposed to severe reaction conditions. The solid-state membranes must provide high oxygen flux, and have a sufficient chemical stability in air and methane environments. A sufficiently low expansion under the operating conditions is desired to sustain the applied mechanical load at high temperatures. Although a lot of compositions are known to satisfy the oxygen flux criterion, these compositions typically do not meet the other above-mentioned demands. For example, mixed conducting oxides reported in the systems Sr(Fe,Co)O_y [6], (Ba,Sr)(Fe,Co)O_y [7], and Ca(Ti,Fe)O_3 [8] do not completely meet the criteria of the membrane materials. High ionic conductivity and high chemical stability in reducing atmospheres at temperatures higher than 700 °C were revealed in perovskites based on lanthanum gallate [9, 10, 11]. Superior electrical and chemical properties make the $LaGaO_3$-based oxides the leading new materials for application in solid oxide fuel cell (SOFC) and methane conversion technologies, and stimulated their further investigation as well [12, 13, 14, 15, 16]. In the perovskite-like oxides ABO_3, wide variation of ionic and electronic constituents of conductivity are possible due to aliovalent substitutions of the host cations in the A and B sites of the crystal lattice. In particular, partial substitution of Sr and Mg for La and Ga, respectively, ensures enhancement of oxygen conductivity up to 0.1 S/cm in solid solutions of (La,Sr)(Ga,Mg)$O_{3-\delta}$ (LSGM) [9, 11].

In this work complex investigation of the structure, microstructure, and dielectric and transport properties of the (La,Sr)(Ga,M)O_y ceramic solid solutions with M = Mg (system I), (Mg,Fe) (system II), and (Mg,Ni) (system III) have been carried out. Changes of the mass- and electrical-transport properties along with the structural characterization of oxides have been made in various atmospheres in a wide temperature range.

Presented at the OSSEP Workshop "Ionic and Mixed Conductors: Methods and Processes", Aveiro, Portugal, 10–12 April 2003

E. D. Politova (✉) · S. Yu. Stefanovich · A. K. Avetisov
V. V. Aleksandrovskii · T. Yu. Glavatskih · N. V. Golubko
G. M. Kaleva · A. S. Mosunov · N. U. Venskovskii
L.Ya. Karpov Institute of Physical Chemistry,
Vorontsovo Pole st. 10, 105064 Moscow, Russia
E-mail: politova@cc.nifhi.ac.ru
Tel.: 095-9173903-123
Fax: 095-9752450

Experimental

Preparation of the samples

Ceramic samples $(La_{1-y}Sr_y)[(Ga_{1-x}Mg_x]O_{3-\delta}$ with x = 0–0.2, y = 0–0.2 (I), $(La_{0.9}Sr_{0.1})[(Ga_{1-x}Fe_x)_{0.8}Mg_{0.2}]O_{3-\delta}$ with x = 0–1.0 (II), and $(La_{0.9}Sr_{0.1})[(Ga_{1-x}Ni_x)_{0.8}Mg_{0.2}]\times O_{3-\delta}$ with x = 0–1.0 (III)

were prepared by two-step solid-state reactions at $T_1 = 970$–1,300 K (6 h) and $T_2 =$ 1,700–1,770 K (1–4 h). Starting materials with chemical grades that ensured the content of main product was not lower than 98% have been used: La_2O_3, Ga_2O_3, MgO, NiO, and $SrCO_3$. The salts $La(NO_3)_3 \cdot 6H_2O$ and $MgCO_3 \cdot Mg(OH)_2 \cdot 3H_2O$ were also tried as precursors in some experiments.

Methods of investigation

The samples were studied by X-ray diffraction ($Cu_{K\alpha}$), electron microscopy (JEOL-35CF), X-ray energy-dispersive microprobe analysis of individual grains and elemental composition (LINK system), and thermogravimetry and dilatometry methods in various gas atmospheres. All the experimental units were computer compatible, PROFITVZ, POWDER, and the standard Microsoft Office programs being used for calculations of the measured characteristics [17]. Two-probe dielectric measurements were carried out at a frequency interval of 1 kHz–1 MHz, in the temperature range 290–1,170 K, using the samples with Pt electrodes that allow evaluation of electronic conductivity by means of dc measurements at low temperatures. Ac current measurements give the values of total ionic plus electronic conductivity. In order to prevent the effects of electrode polarization, bar-like samples with dimensions 1.5×1.5×8 or 3×3x7 mm were used for the conductivity measurements with the smallest-area faces of the bars being attached to the electrodes.

Table 1 Element composition of grains in $La_{0,.8}Sr_{0,.2}Ga_{0,.83}Mg_{0,.17}O_{2,.815}$ (LSGM_1), $La_{0.8}Sr_{0.2}Ga_{0.8}Mg_{0.2}O_{2.8}$ (LSGM_2), and $(La_{0.9}Sr_{0.1})[(Ga_{1-x}Ni_x)_{0.8}Mg_{0.2}]O_{3-\delta}$(Ni_0.4, Ni_0.6, Ni_1.0) according to the results of the energy- dispersive X-ray microanalysis, normalized to B site concentration. "A" letters markindicates analysis of areas 600x×450 μm, "B" – indicates analysis of individual grains with size ~1,.5÷–10 μm

Composition, x	La (±0.02)	Sr (±0.02)	Ga (±0.03)	Ni (±0.03)	Mg (±0.02)
LSGM_1					
A	0.88	0.21	0.76	–	0.24
A	1.03	0.21	0.82	–	0.18
B (1:1)	0.84	0.18	0.79	–	0.21
B (3:2)	1.19	0.22	0.82	–	0.18
B (3:2)	1.12	0.21	0.81	–	0.19
LSGM_2					
A	0.71	0.145	0.82	–	0.18
B (1:1)	0.845	0.11	0.82	–	0.18
B (1:1)	0.47	0.43	0.97	–	0.03
B (3:2)	0.73	0.58	0.89	–	0.11
B (3:2)	0.79	0.61	0.88	–	0.12
Ni_0.4					
A	0.92	0.11	0.44	0.40	0.16
B	0.77	0.10	0.47	0.39	0.15
B (1:1)	0.89	0.12	0.33	0.51	0.16
Ni_0.6					
A	0.89	0.14	0.29	0.60	0.11
B (3:2)	1.16	0.16	0.19	0.75	0.06
B (3:2)	1.08	0.17	0.20	0.685	0.11
B (1:2)	0.27	0.19	0.51	0.35	0.13
Ni_1.0					
A	1.42	0.13	0.07	0.84	0.09
B (2:1)	1.71	0.26	0.13	0.87	0
B (2:1)	1.76	0.15	0	1.00	0
B (2:1)	1.68	0.28	0	1.00	0
B ($MgNiO_2$)	0	0	0	0.56	0.44
B (3:2)	1.28	0.08	0	1.00	0

Results and discussion

Phase content, structure, and microstructure parameters

The perovskite-like phase is the main phase in samples of I, though small contents (< 1%) of various admixture phases such as La_4SrO_7, $La_2SrO_{4+\delta}$, and (La,Sr)GaO_3 are also often detected using X-ray and electron microprobe analysis (Table 1) [18, 19]. According to the X-ray diffraction patterns, change of the unit cell symmetry from orthorhombic (at $0 < x + y < 0.3$) to rhombohedral (at $0.3 \le x + y \le 0.35$) and finally to cubic (at $x + y > 0.35$) takes place (Fig. 1). However, the symmetry of the latter composition is really lower than cubic, as it follows from IR [18], Raman [20], and electron diffraction [21] data. This discrepancy may be explained by the fact that the X-ray diffraction method registers only the mean macroscopic symmetry of the tested samples. In reality, there is evidence of lattice relaxation and ion ordering effects, that can lead to formation of the different symmetry nanoscale domains and further phase separation in compositions with a high number of the vacant anion sites.

Taking into account the highest values of the LSGM ionic conductivity reported, the composition containing 10 and 20% of Sr and Mg, respectively, in the A and B sites of the perovskite lattice has been chosen as the base composition for systems II and III [9, 11]. Substitution of iron or nickel for gallium ensures contraction of the rhombohedral perovskite unit cell with increasing Fe cation content up to ~30%, and with increasing Ni cation content up to 50% (Fig. 2). On increasing the Fe content further, the unit cell volume grows.

In system III, a mixture of the perovskite solid solution, the tetragonal phase $(La,Sr)_2NiO_4$ and cubic phase $MgNiO_2$ were revealed in the samples with $x > 0.4$ (Table 1). These data allow us to testify the substitution of Ni^{3+} for Ga^{3+} in the perovskite compositions with $x < 0.5$ in system III. The observed contraction of unit cell volume is explained by the substitution of the Fe^{4+} cations for Ga^{3+} at $x < 0.3$ in system II. Substitution of the high spin configuration Fe^{3+} ions for Ga should be assumed in order to explain the observed increase of the unit cell volume at $x > 0.4$.

The mean size of grains in the ceramics studied varied from 10–50 μm in pure $LaGaO_3$ ceramics to 1–3 μm in the LSGM and the Fe- and Ni-doped ceramics (Fig. 3).

Mass changes

On heating up to 870 K, negligible mass losses $\Delta m/m$ have been detected in all the ceramics I–III (Fig. 4). With further temperature increase, noticeable mass losses have been revealed in the LSGM samples doped with Fe or Ni. The observed difference in the mass loss for samples with various concentrations of Fe or Ni ion may be explained by the different content of the oxygen

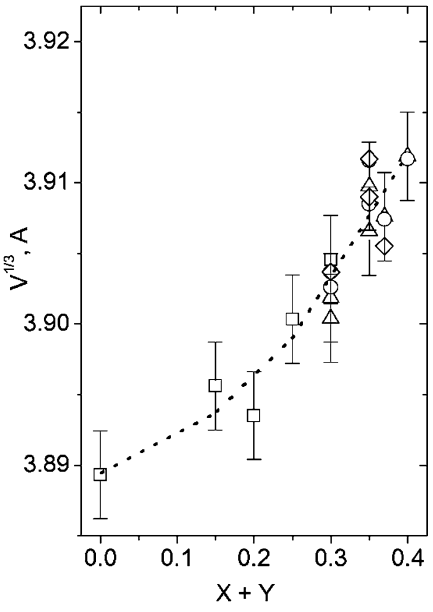

Fig. 1 The unit cell parameter $\bar{a} = V^{1/3}$ as a function of concentration of the substituting Sr and Mg cations $(x+y)$ in the samples $(La_{1-y}Sr_y)[(Ga_{1-x}Mg_x]O_{3-\delta}$

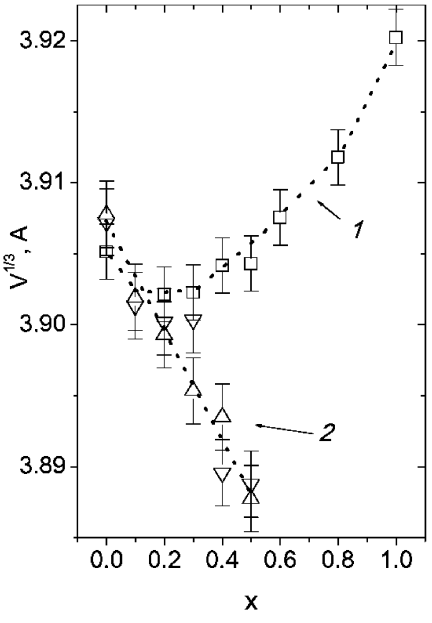

Fig. 2 The unit cell parameter $\bar{a} = V^{1/3}$ as a function of concentration x of the substituting cations in the $(La_{0.9}Sr_{0.1})[(Ga_{1-x}Fe_x)_{0.8}Mg_{0.2}]O_{3-\delta}$ (*curve 1*) and $(La_{0.9}Sr_{0.1})[(Ga_{1-x}Ni_x)_{0.8}Mg_{0.2}]O_{3-\delta}$ (*curve 2*) systems

species weakly associated with iron or nickel ions in the lattice. In both systems, the highest mass losses have been observed for the samples with $x = 0.2$–0.3. This correlates with nonlinear unit cell parameter behavior, conditioned by variations in the transition element valence and pointing to a maximum concentration of weakly bonded high-valence species at the same x values (Fig. 5).

Thermal expansion

Similarly, the dilatometry curves $\Delta L/L(T)$ measured for samples II and III revealed linear temperature dependence up to ~870 K on heating in air (Fig. 6). With further heating, additional expansion, evidently due to the effect of oxygen vacancy creation, contributes to the ordinary linear thermal expansion of the lattice. Calculated for the temperature interval near 1,070 K, the thermal expansion coefficient α reveals maximum values $\sim(16 \pm 1)\cdot 10^{-6}$ 1/K (II) and $\sim(22 \pm 1)\cdot 10^{-6}$ 1/K (III) at $x = 0.3$–0.5 and 0.2–0.4, respectively (Fig. 7). At higher concentrations, the α values slightly decrease being practically constant in the samples with $x > 0.6$. This result evidently confirms that more stable oxygen species are being provided when the concentration of the Fe or Ni cations increases.

The mass and linear expansion changes were also studied for samples of III with $x = 0.4$ during a reduction–oxidation cycle. The $\Delta m/m$ changes turned out to be completely reversible with heating (up to 1,170 K)–cooling cycles beginning in air, then in nitrogen and finally, in oxygen atmospheres. The $\Delta L/L$ value did not change when the atmosphere was reversed from nitrogen to oxygen at temperatures lower than 970 K, while a slight ~0.04% contraction of dimensions happened when the nitrogen atmosphere was reversed to oxygen at 1,120 K.

Conductivity measurements

The ac conductivity values of samples of I increase with increasing electric field measuring frequency at temperatures < 770 K, while they do not depend on measuring frequency at higher temperatures. The observed feature may be explained by the dielectric relaxation effect that is confirmed to contribute to the low-frequency conductivity values in the low-temperature region [19, 22]. According to the Debye model, displacement of charged ion species in the lattice corresponds to electrical dipole creation. We observed characteristic peaks in the dielectric loss and dielectric permittivity versus temperature curves. The peaks shift to higher temperature with increasing measuring frequency. Moreover, straight lines were found to describe the frequency–temperature dependences for the peaks on $\tan\delta(T)$ and $\epsilon(T)$ curves in coordinates ln f versus $1/T$ and ln $f/T^{1/2}$ versus $1/T$, respectively, for all the samples of I studied. This supports the validity of the approach used and allows evaluation of relaxation parameters. The size of the relaxing dipoles l was estimated as $l \approx 0.7$ Å. The l value obtained is essentially lower than the distance between the oxygen positions in the lattice (~2.75 Å). This has allowed the conclusion that correlated movement of oxygen vacancies is possible at temperatures lower than 770 K [15]. This conclusion agrees with the computer simulation results on cluster formation in perovskite-type oxide [23].

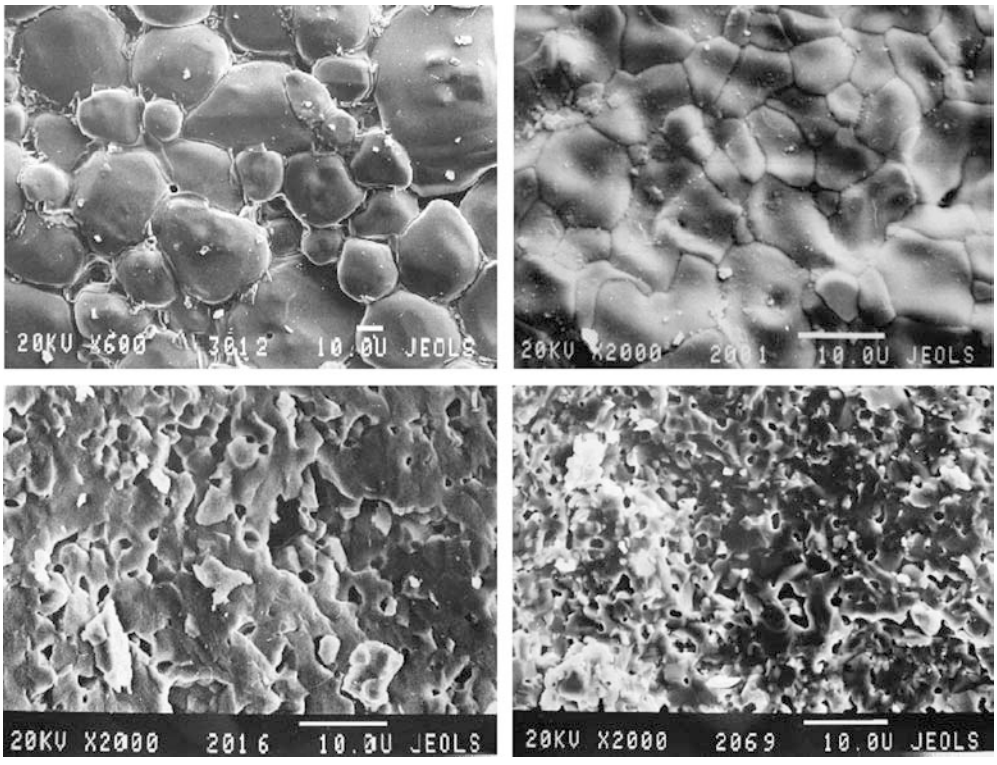

Fig. 3 Electron micrographs of surface of the samples: $(La_{1-y}Sr_y)[(Ga_{1-x}Mg_x]O_{3-\delta}$ with x, $y=0$ (*top left*), $x=0.2$, $y=0.1$ (*top right*) (as fired surfaces); $(La_{0.9}Sr_{0.1})[(Ga_{1-x}M_x)_{0.8}Mg_{0.2}]O_{3-\delta}$ with M = Fe, $x=0.4$ (*bottom left*), M = Ni, $x=1.0$ (*bottom right*) (fracture surfaces)

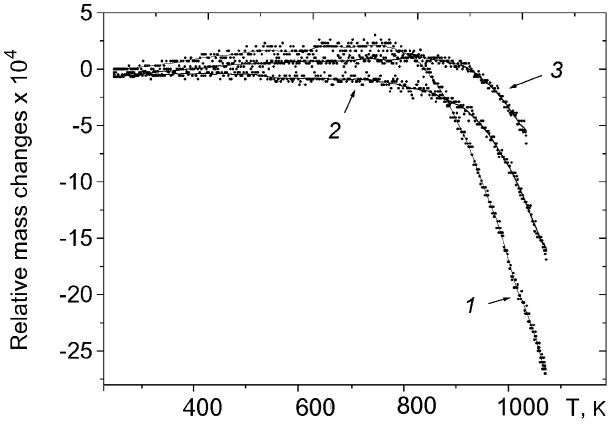

Fig. 4 The mass change as a function of temperature on heating in air for the samples $(La_{0.9}Sr_{0.1})[(Ga_{1-x}Ni_x)_{0.8}Mg_{0.2}]O_{3-\delta}$ with $x=0.2$ (*1*), 0.5 (*2*), 0.6 (*3*)

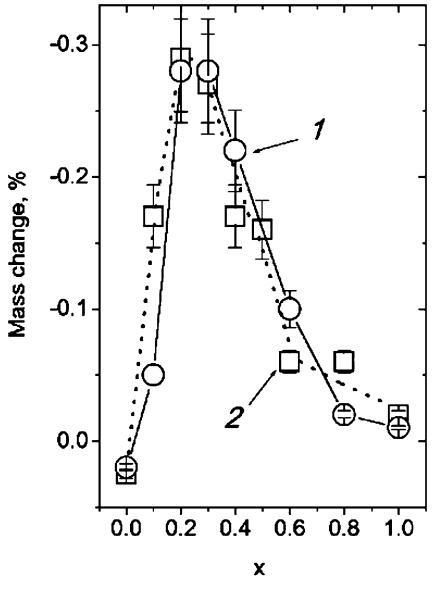

Fig. 5 The mass loss measured in the temperature range 650–800 °C as a function of concentration x of M = Fe (*curve 1*) or M = Ni (*curve 2*) cations for the samples $(La_{0.9}Sr_{0.1})[(Ga_{1-x}M_x)_{0.8}Mg_{0.2}]O_{3-\delta}$

At temperatures higher than 770 K, the ac conductivity follows the Arrhenius law with the activation energy $E_a = 0.7$–1.4 eV.

The electronic part of the conductivity σ_e, estimated by dc measurements, is low for the pure ionic (oxygen) conducting compositions I and for the ceramics II and III with $x=0$. σ_e values are much lower than 10^{-8} S/cm at room temperature, while they increase up to $\sim 5 \cdot 10^{-3}$ S/cm at 1,000 K. Introduction of Fe or Ni cations ensures a total conductivity increasing up to ~2 orders of magnitude at ~1,000 K, with σ_e increasing to more than 5–7 orders of magnitude at room temperature and up to ~4 orders of magnitude at 1,000 K (Figs. 8, 9).

According to the results obtained, the perovskite structure phase is the dominant one in samples I and II at all values of x and at $x<0.5$ in samples of III. Namely, in the compositions II and III with $0.1<x<0.4$ the electronic constituent of conductivity increases significantly. So, the observed transition from pure ionic to the mixed ionic–electronic conductivity is evidently

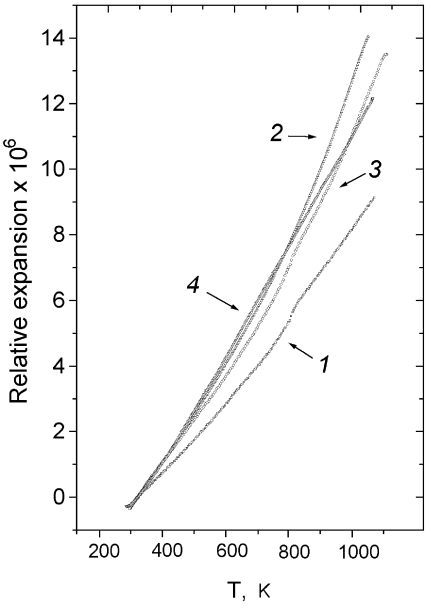

Fig. 6 The relative linear expansion as a function of temperature for the samples $(La_{0.9}Sr_{0.1})[(Ga_{1-x}Ni_x)_{0.8}Mg_{0.2}]O_{3-\delta}$ with $x=0$ (*1*), 0.3 (*2*), 0.4 (*3*), 0.8 (*4*)

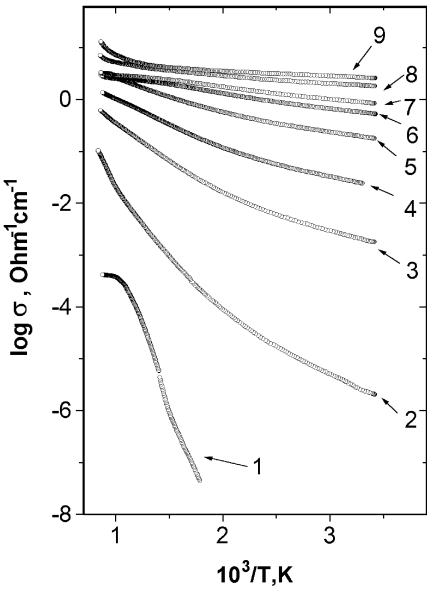

Fig. 8 Dc conductivity as a function of the reciprocal temperature for the samples $(La_{0.9}Sr_{0.1})[(Ga_{1-x}Ni_x)_{0.8}Mg_{0.2}]O_{3-\delta}$ with $x=0$ (*1*), 0.1 (*2*), 0.2 (*3*), 0.3 (*4*), 0.4 (*5*), 0.5 (*6*), 0.6 (*7*), 0.8 (*8*), 1.0 (*9*)

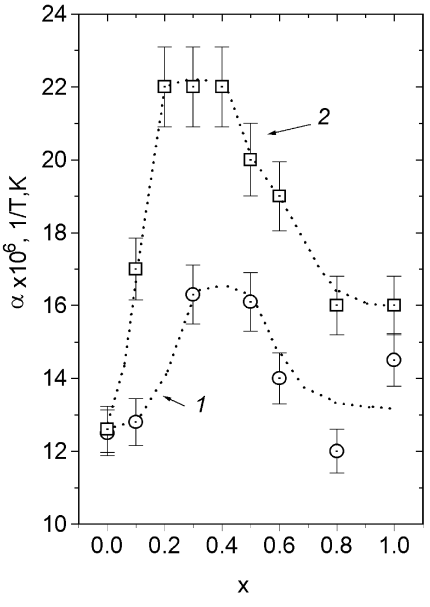

Fig. 7 Coefficient of thermal expansion $\alpha = d(\Delta L/L)/dT$ calculated at 1,070 K as a function of concentration x for the samples $(La_{0.9}Sr_{0.1})[(Ga_{1-x}M_x)_{0.8}Mg_{0.2}]O_{3-\delta}$ with M = Fe (*curve 1*) or M = Ni (*curve 2*)

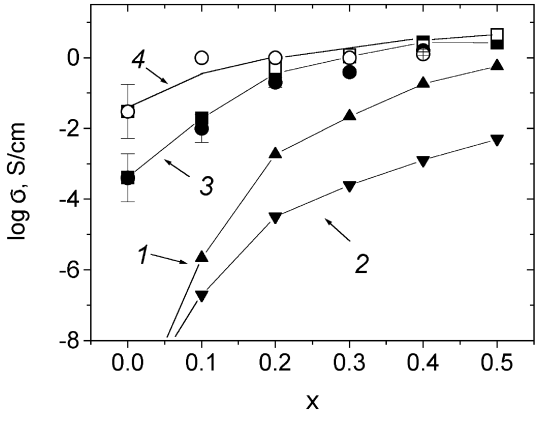

Fig. 9 Dc (*solid*) and ac (*open*) conductivity values measured at room temperature (*1*, *2*) and at 1,000 K (*3*, *4*) as a function of concentration x for $(La_{0.9}Sr_{0.1})[(Ga_{1-x}Fe_x)_{0.8}Mg_{0.2}]O_{3-\delta}$ ceramics (*circles*, *up triangles*), and for $(La_{0.9}Sr_{0.1})[(Ga_{1-x}Ni_x)_{0.8}Mg_{0.2}]O_{3-\delta}$ ceramics (*squares*, *down triangles*)

provided by substitutions in the perovskite-phase solid solutions. It is also clear that high σ_e values ≥1 S/cm, which are sufficient for practical use of the oxides as membrane materials, can be easily reached at high temperatures in the Fe- or Ni-doped ceramics.

Bearing in mind the enhancement of the ionic conductivity with the increasing concentration of oxygen vacancies, and taking into account the observed mass loss, we may assume the preservation of ionic conductivity at a level $\sigma_i \sim 0.1$ S/cm in the compositions II and III with $x < 0.4$. The σ_i values are lower than the σ_e values, so in the sense of application, ionic conductivity should be improved. The improvement may be achieved in the pure phase ceramics of high density prepared using wet chemical methods [24].

The results of the study confirm the possibility of regulation of conductivity in compositions II and III. As the conductivity values at high temperatures are similar (Fig. 9), the compositions studied may be considered as promising for development of membrane materials. It is

also worth noting that the Ni-composed catalysts may be used in the methane conversion reactor [16].

Conclusions

The results obtained confirm formation of solid solutions in the whole range of concentrations in the case of Fe substitutions, with multiphase compositions in the Ni-containing ceramics III with $x > 0.5$. Transformation from pure ionic conductivity to mixed ionic–electronic conductivity in the perovskite (La,Sr)(Ga,M,Mg)O_y oxides with M = Fe or Ni has been observed. Mass losses were proved to correlate with the thermal expansion coefficient and electrical transport properties. The properties of the ceramics studied point to their prospects for development of membrane materials for methane conversion.

References

1. Riess I (1992) Solid State Ionics 52:127
2. Bonanos N, Knigh KS, Ellis B (1995) Solid State Ionics 79:161
3. Dresselhaus MS, Thomas IL (2001) Nature 414:332
4. Steele BCH, Heinzel A (2001) Nature 414:345
5. Balachandran U, Dusec JT, Sweeney SM (1995) Am Ceram Soc Bull 74:71
6. Mitchell BJ, Richardson JW, Murphy CD (2000) Mater Res Bull 35:491
7. Shao Z, Yang W, Cong Y, Dong H (2000) J Memb Sci 172:177
8. Esaka T, Fujii T, Suwa K, Iwahara H (1990) Solid State Ionics 40/41:544
9. Ishihara T, Matsuda H, Takita Y (1994) J Am Chem Soc 116:3801
10. Ishihara T, Matsuda H, Takita Y (1995) Solid State Ionics 79:147
11. Huang P, Petric A (1996) J Electrochem Soc 143:1644
12. Baker RT, Gharbage B, Marques FMB (1997) J Electrochem Soc 144:3130
13. Trofimenko N, Ulmann H (1999) Solid State Ionics 118:215
14. Kharton VV, Yaremchenko AA, Viskup AP, Mather GC, Naumovich EN, Marques FMB (2000) Solid State Ionics 128:79
15. Huang K, Tichy R, Goodenough JB (1998) J Am Ceram Soc 81:2565
16. Ishihara T, Hiei Y, Takita Y (1995) Solid State Ionics 79:371
17. Zhurov VV, Ivanov SA (1997) Kristallografiya 42:239 (in Russian)
18. Aleksandrovskii VV, Venskovskii NU, Kaleva GM, Politova ED, Prutchenko SG, Rudnitskii LA, Stefanovich SYu, Khortova AYu (2001) Inorg Mater 37:641 (translation from Russian)
19. Glavatskikh TYu, Venskovsky NU, Kaleva GM, Mosunov AV, Politova ED, Stefanovich SYu (2001) Inorg Mater 37:764 (translation from Russian)
20. Inagaki T, Miura K, Yoshida H, Fujita H (1999) Solid State Ionics 118:265
21. Mathews T, Sellar JR (2000) Solid State Ionics 135:411
22. Aleksandrovskii VV, Venskovskii NU, Kaleva GM, Mosunov AV, Politova ED, Stefanovich SYu, Avetisov AK (2001) Bull Russ Acad Sci Phys 65:1237
23. Islam MS (2002) Solid State Ionics 154–155:75
24. Feng M, Goodenough JB (1996) J Am Ceram Soc 79:1100